

Rheology and Molecular Weight Changes during Enzymatic Degradation of a Water-Soluble Polymer

Akash Tayal, Robert M. Kelly, and Saad A. Khan*

Department of Chemical Engineering, North Carolina State University,
Raleigh, North Carolina 27695-7905

Received May 14, 1998; Revised Manuscript Received November 5, 1998

ABSTRACT: The rheological behavior and molecular weight characteristics of a natural polymer undergoing enzymatic hydrolysis were examined for aqueous guar solutions. Changes in weight-average molecular weight (M_w), deduced from gel permeation chromatography (GPC), were used to construct a kinetic model for the process, such that $1/M_w \propto kt$, with the rate constant, k , varying inversely with polymer concentration. This relationship suggests that enzymatic degradation was zeroth-order in guar concentration. These findings contrast with previous studies of natural polymer degradation which usually have interpreted the linear relationship between $1/M$ and time as first-order processes. Our analysis reveals that this linear relationship is expected regardless of the reaction order and that the true order can be determined only from the dependence of the degradation rate on initial polymer concentration. Rheological properties were sensitive to extent of degradation; several orders of magnitude change in zero shear viscosity were observed over the course of polymer chain scission. Moreover, the viscosity–time profiles for different enzyme concentrations could be collapsed onto a single curve by temporal scaling. This could be used to predict, a priori, guar solution viscosity as a function of degradation time and enzyme concentration. This “concentration–degradation time” superposition was based on a unique relationship between zero shear viscosity, η_0 , and the product of enzyme concentration and degradation time.

Introduction

The enzymatic hydrolysis of natural polymers is a complex phenomenon, which involves significant changes in solution viscosity as the macromolecule is progressively degraded into smaller molecular units. Enzymatic access to cleavage sites on the polymer can be influenced by polymer concentration, solution viscosity, and the presence of appendages to the backbone. Controlling the extent of enzymatic hydrolysis can be important, if specific rheological properties of the biopolymer solution are required. Thus, insights into how this process proceeds and how it might be manipulated are important.

Guar galactomannan is a water-soluble polysaccharide consisting of a linear backbone of β -1,4-linked mannose units with α -1,6-linked galactose units as side chains, the ratio of mannose to galactose units being $\sim 1.6:1$.^{1,2} Guar is used extensively in industry due to its excellent viscosifying properties and low cost.^{3,4} In many of its applications, however, the chemical architecture or chain size of the guar molecule needs to be modified. For example, guar degraded to yield a lower galactose (side chain) content can be utilized to form synergistic gels with biopolymers such as xanthan and κ -carrageenan in various food applications.⁵ In the oil and gas industry, guar is used with sand (proppant) to fracture oil- or gas-bearing rock in a process known as hydraulic fracturing. Subsequently, the guar gel needs to be degraded, preferably in a controlled manner, to facilitate oil and gas flow.^{6,7} In both these applications, enzymes offer a convenient and efficient way to degrade and hydrolyze the galactomannan. However, critical to the use of enzymes is a fundamental understanding of

the degradation kinetics and their impact on the rheological properties of guar formulations, both of which are presently lacking.

Previous studies on guar galactomannans have essentially focused on *nondegraded* solutions and gels.^{6–10} Recently, however, the effects of process variables such as temperature, pH, and enzyme concentration on guar solution degradation have been investigated using steady shear rheological measurements.¹¹ Solution viscosity was found to be very sensitive to extent of guar hydrolysis and decreased by several orders of magnitude during the course of degradation. The extent of viscosity reduction was controlled by a balance between thermostability and thermoactivity of the enzyme. As a result, an optimum temperature for enzyme efficacy was observed. In this study, the molecular properties of guar galactomannan solutions during enzymatic degradation were investigated and related to rheological characteristics. Information gained from gel permeation chromatography (GPC), concerning patterns of molecular weight distribution during hydrolysis, was used to determine the kinetics for the degradation reaction. Reduction in steady shear viscosity during hydrolysis was also followed and related to molecular weight distribution patterns. By correlating the two approaches, insights into the degradation process that cover molecular to macroscopic scales are obtained, leading to a better understanding of enzymatic guar degradation.

Experimental Section

Materials. Food-grade guar galactomannan (Jaguar 6003, Rhone-Poulenc, NJ) was purified through Soxhlet extraction with ethanol.¹² Solutions were prepared by dispersing purified guar powder in a sodium phosphate buffer.¹¹ Additionally, solutions were centrifuged at 20 000*g* for 1.5 h to obtain a clarified solution. Enzymatic guar degradation was performed using Gamanase, a commercial hemicellulosic extract from

* To whom correspondence should be addressed. Ph (919)-515-4519; Fax (919)-515-3465; e-mail khan@eos.ncsu.edu.

Aspergillus niger, containing primarily a mixture of endo- β -mannanase and α -galactosidase (Novo Nordisk Bioindustrials, Inc., Franklinton, NC). Over the time frames of the experiments reported here, the influence of α -galactosidase on chain breaking was found to be insignificant (data not shown). As such, biopolymer degradation is assumed to result from β -mannanase activity. This is supported by McCleary,¹³ who reports that α -galactosidase derived from fungal sources, as in Gammanase, is inert toward cleaving guar; the only α -galactosidases that can remove D-galactose from guar are those derived from seed sources (e.g., guar), a result which has been verified in our laboratory.¹⁴ Enzymatic hydrolysis was performed on 0.5 and 1 wt % guar solutions at 25 °C and pH of 6.5. Enzyme activity was determined by using the following protocol for RBB-Carob Galactomannan as substrate. Enzyme solution (0.25 mL) was added to preequilibrated substrate solution (0.5 mL) prepared according to the Megazyme mannanase assay procedure (Megazyme, Sydney, Australia). Solutions were mixed and incubated at 40 °C for 30 min. One milliliter of ethanol (95% v/v) was then added, and the tubes were vigorously mixed on a vortex stirrer for 10 s, at which time the high molecular weight, nonhydrolyzed, dyed galactomannan precipitated. The reaction tubes were then centrifuged at 12 000 rpm in a microcentrifuge (Sorvall MC12V, DuPont, Wilmington, DE) for 10 min. The supernatant was poured directly into a cuvette in the spectrophotometer cell, and the absorbances of the reaction and of the blank were read against distilled water at 590 nm. Activity was defined as μmol of mannan released/min, calculated by reference to a standard curve.

GPC Measurements. Molecular weight (MW) averages and molecular weight distributions (MWD) were determined by GPC on a bank of Ultrahydrogel columns (Ultrahydrogel 2000, 500, and 120, Waters Corp., Milford, MA). A guard column (Ultrahydrogel Guard Column, Waters) was placed ahead of the column bank. A Shimadzu HPLC system with RID-6A differential refractive index detector was used. The mobile phase was water containing 0.1 M sodium nitrate and 5×10^{-3} M sodium azide; the flow rate was fixed at 0.8 mL/min, and a temperature of 45 °C was used. All degraded guar samples were diluted to 0.05%–0.1% (w/v) (to eliminate viscous spreading in the columns) and filtered through 0.45 μm filter prior to analysis. The dilution was made in 4 M urea solution, which also served to denature the enzyme and stop the degradation reaction. The bank of columns was calibrated using the pullulan standards. Eight fractions of pullulan ranging from molecular weights of 5200 to 1.6 million were used as standards (Shodex Corp., Japan). Pullulan solutions were prepared in deionized water (Millipore, Bedford, MA), as prescribed by company literature. The MW distributions thus obtained were checked for skewing and symmetrical spreading using the ASTM method D3536-91. Both effects were found to be small and were neglected. GPC separates the molecules on the basis of their hydrodynamic size; molecules of identical hydrodynamic volume (but not necessarily molecular weight) elute at the same time. Thus, the molecular weights obtained by comparison with standards (of known molecular weight) are relative and not absolute. A universal calibration procedure can be applied to calculate absolute molecular weight distributions from chromatographic data and has been shown to be applicable for nonionic polysaccharides.^{15,16} Thus, for universal calibration, hydrodynamic volumes of guar and the standards (pullulan) are equated to give

$$[\eta]_g M_g = [\eta]_p M_p$$

where $[\eta]$ is the intrinsic viscosity; the subscripts g and p refer to guar and pullulan, respectively. The following data from literature were used for intrinsic viscosity values:

$$[\eta]_g = 3.8 \times 10^{-2} M_g^{0.723} \text{ (cc/g) (from ref 16)}$$

$$[\eta]_p = 1.9 \times 10^{-2} M_p^{0.67} \text{ (cc/g) (from ref 10)}$$

Thus,

$$M_g = 0.67 M_p^{0.97}$$

The molecular weight averages were calculated by numerical integration of the MW distribution curve. The reproducibility in the MW averages was within $\pm 2\%$.

Viscosity Measurements. Required amounts of enzyme were injected into a preequilibrated guar solution that was incubated at 25 °C. Aliquots were withdrawn after specified time periods and tested on a stress-controlled rheometer (DSR II, Rheometrics, Piscataway, NJ). Steady stress viscosity measurements were made using a couette geometry with inner bob and outer cup radii of 14.75 mm and 16.0 mm, respectively, and a bob length of 44.25 mm.

Results and Discussion

Molecular Weight Reduction for Enzymatically Modified Guar. Figure 1 shows typical molecular weight distribution patterns for 1% (w/v) guar galactomannan solutions, degraded to different extents at 25 °C and pH of 6.5. Results corresponding to different extents of hydrolysis (2 and 13 h) are shown and compared to nondegraded guar. Significant reduction in molecular weight is observed during the course of the enzymatic hydrolysis, with the peak maximum shifting by almost 2 orders of magnitude. This reflects the cleavage of backbone linkages by the endo-acting β -mannanase since the α -galactosidase has no effect on guar degradation.^{13,14} Additionally, the molecular weight distributions (MWD) broaden considerably with time. MWD data could be integrated to obtain average molecular weights, such as M_n (number-average MW) and M_w (weight-average MW), of guar during enzymatic hydrolysis. Figure 2 shows such a plot of the changes in M_n and M_w with degradation time. The reduction in both M_n and M_w is rapid at short times but slower subsequently.

The time-dependent MWD patterns can be interpreted using rate functions to obtain the order of the enzymatic degradation reaction. Historically, first-order kinetics have been used to describe polymer degradation kinetics.^{17–22} This is given by

$$dL/dt = -kL \quad (1)$$

where the total number of hydrolyzable linkages, L , reduces at a rate (dL/dt) that is directly proportional to L , with a rate constant k . There are $(M/m - 1)$ linkages per molecule, where M is the average molecular weight of the chain and m is the monomer molecular weight. Thus, by substituting $L = N_0(M/m - 1)$ for N_0 total molecules in eq 1 and considering $(m/M) \ll 1$, the following relation between molecular weight and degradation time can be obtained.

$$\frac{1}{M_t} = \frac{1}{M_0} + \frac{kt}{m} \quad (2)$$

In this expression M_t and M_0 are the molecular weights at time t and time zero, respectively. This linear relation between inverse molecular weight and degradation time has since been used as evidence for first-order kinetics for a variety of systems, including thermal degradation of polycarbonate solutions,¹⁹ as well as acid hydrolysis of cellulose²³ and carageenans.^{20,24,25} Although initially developed for number-average molecular weight (M_n), eq 2 has been shown to hold for weight-average molecular weight (M_w).¹⁸

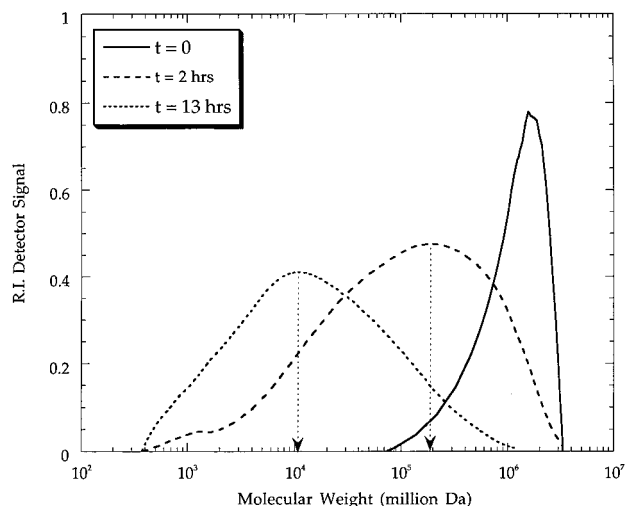


Figure 1. Typical chromatograms for guar solutions degraded to different extents at 25 °C and solution pH of 6.5. The enzyme activity was 2.5×10^{-3} U/mL of 1% guar solution.

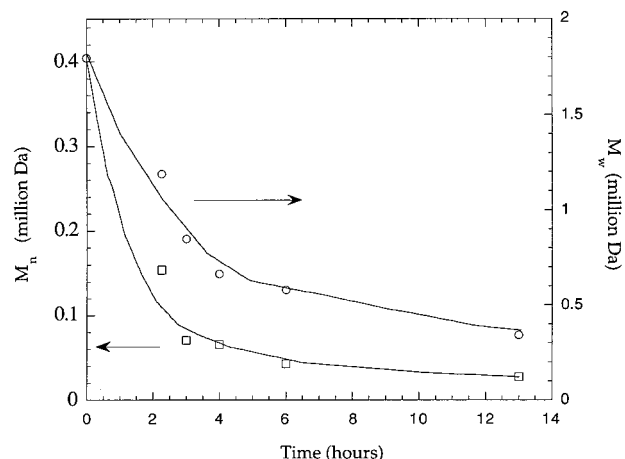


Figure 2. Changes in number- and weight-average molecular weights, M_n and M_w , of guar solutions as a function of degradation time. Enzyme concentration was 8.4×10^{-4} U/mL of 1% guar solution.

To examine whether guar degradation followed first-order kinetics, the inverse weight-average molecular weight ($1/M_w$) of guar has been plotted as a function of degradation time for enzymatic hydrolysis of 0.5% and 1% (w/v) guar solutions (Figure 3). Here, M_w instead of M_n is used because M_w is a better representation of the high molecular weight fraction that controls rheological behavior,²⁶ which then facilitates subsequent correlation of molecular changes with the rheological properties. Figure 3 reveals a linear relationship between $1/M_w$ and t for guar system, consistent with eq 2, and it appears that the first-order analysis should apply in this case. However, the slope of $1/M_w$ vs time, which is related to the apparent rate constant k , decreases as guar concentration increases from 0.5% to 1%. For a first-order process, k should be independent of the total number of guar linkages, L , which is directly proportional to the initial polymer concentration. There is, therefore, an apparent anomaly here in that, although the degradation reaction appears to be first order, the rate constant is dependent on polymer concentration. Such an inconsistency can be resolved by generalizing the degradation reaction (eq 1) to be an n th-order process:²⁷

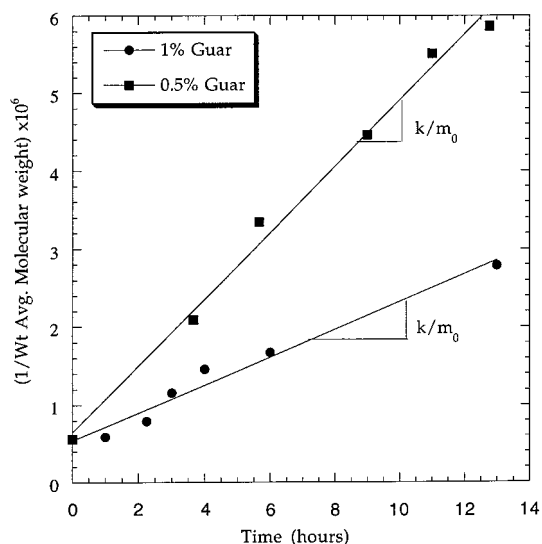


Figure 3. Reciprocal of weight-average molecular weight, M_w , plotted as a function of degradation time. Enzyme concentration was same as that for Figure 2.

$$dL/dt = -kL^n, \text{ where } n \text{ is the order of reaction} \quad (3)$$

By integrating and making appropriate substitutions, the following result is obtained:

$$\left[\left(1 - \frac{m}{M}\right)^{1-n} - \left(1 - \frac{m}{M_0}\right)^{1-n} \right] = \frac{k(n-1)}{N_0^{1-n}} t$$

Thus, for zeroth order, $n = 0$,

$$\frac{1}{M} = \frac{1}{M_0} + \frac{k}{mN_0} t \quad (4)$$

And, for second order, $n = 2$,

$$\frac{1}{M} \approx \frac{1}{M_0} + \left(\frac{kN_0}{m} \right) t \quad (5)$$

Here, c_0 is the initial concentration of guar. The approximation made for the second-order case is similar to that made for the first-order analysis and is valid as long as the degradation is not carried out to the extent that only very small guar molecules remain.

Equations 2, 4, and 5, therefore, reveal that, regardless of the order of the reaction, the same functional dependence of molecular weight on degradation time is predicted for zero-, first-, and second-order degradation reactions. In fact, this will also hold true for higher-order reactions (third and higher; see Appendix for details). The true order of reaction can be determined only by examining the effect of initial polymer concentration, c_0 , on the apparent rate constant, S (slope of $1/M_w$ versus time plot). In general, for a reaction of order n ,

$$S = \frac{kN_0^{n-1}}{m}$$

Substituting

$$c_0 = \frac{N_0 V}{N_{av} m}$$

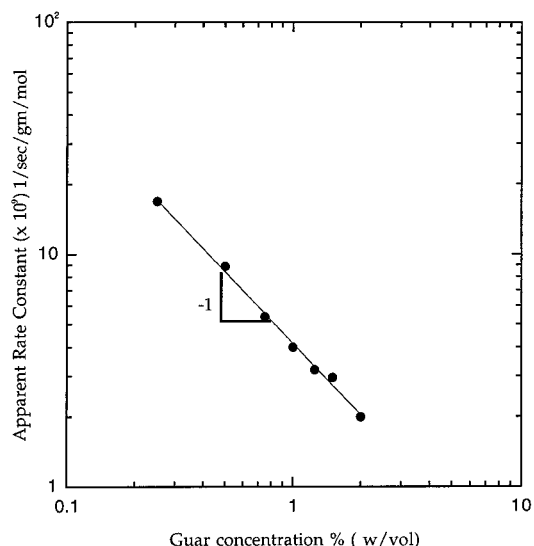


Figure 4. Apparent rate constant as a function of guar concentration. Enzyme concentration same as that for Figure 2.

where N_{av} is the Avogadro number and V the sample volume, we get

$$S \sim c_0^{n-1}$$

Thus, for a zero-order reaction, the slope is proportional to $(1/c_0)$. Indeed, this is what is observed for this system. A plot of the apparent rate constant as a function of guar concentration demonstrates an inverse dependence (Figure 4), confirming that the degradation is zeroth order in guar concentration. For a first-order reaction, S should be independent of c_0 . It is, therefore, critical that the relationship between S and c_0 is checked before any conclusions on reaction kinetics are made. Only a few studies have resorted to this "consistency check" to ensure validity of their analyses.^{25,27}

A physical explanation of the observed zeroth-order degradation rate emerges upon considering the relative concentrations of guar and biocatalyst present in the system. Here, the guar concentration is 10 g/L, and the corresponding concentration of mannose linkages is 0.04 M (MW of mannose = 162, ratio of galactose to mannose of 1:1.6). The enzyme concentration is $\sim 10 \mu\text{g/L}$ or 0.2×10^{-9} M (MW of 42 000 for the monomeric β -mannanase).²⁸ Under these conditions, there are sufficient substrate sites so that every enzyme molecule has bound a molecule of substrate to form an enzyme-substrate complex. Thus, increasing the substrate concentration cannot increase the number of complexes formed. As a result, the rate of scission of guar linkages is unchanged, implying that the degradation is zeroth-order in linkage (or guar) concentration. Similar kinetic behavior is observed for enzymatic catalysis of simple substrates at high substrate/enzyme ratios and is termed "substrate saturation". This zeroth-order kinetics are modeled well by classical Michaelis-Menten kinetics. However, there is a subtle point that begs to be raised. As noted in the Introduction, the fact that we have an enzyme-polymer system changes the nature of the degradation process as compared to a typical enzyme-substrate (small molecule) reaction. Indeed, the kinetics of the action of mannanase enzyme on a simple substrate as well as on galactomannan have been investigated by McCleary and Matheson²⁹ using the traditional

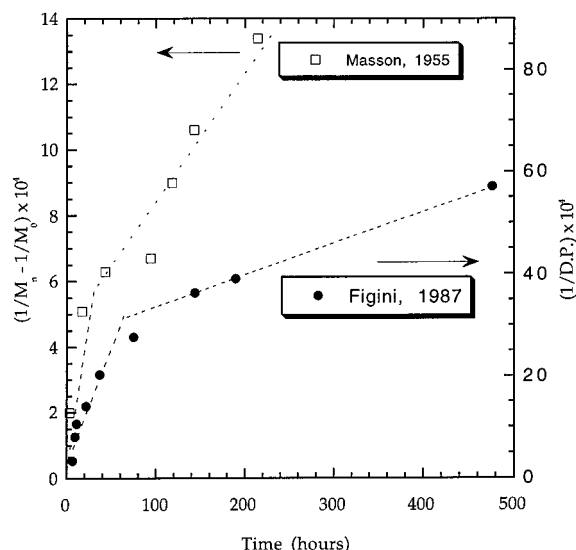


Figure 5. Inverse of number-average molecular weight as a function of time for acid hydrolysis of carrageenan (reproduced from ref 24) and 1/DP (degree of polymerization) as a function of time for acid hydrolysis of cellulose (reproduced from ref 23).

Michaelis-Menten approach. Their results show different values of the constants (K_m and V_{max}) for galactomannan (polymer) vs mannohexaitol (oligosaccharide, small substrate). Thus, the precise mechanistics of degradation is considerably different for a polymer than a small molecule.

The analysis provided here is also relevant for complex reactions where the kinetic mechanism can be a combination of two or more reactions with different orders. This is illustrated through Figure 5 which shows the inverse molecular weight ($1/M$) as a function of time for two cases: the acid hydrolysis of cellulose²³ and carrageenan.^{24,25} Both sets of data display two distinct kinetic regimes that have not been fully elucidated. Usually, the initial phase is ignored, and first-order kinetics are assumed to apply for the second phase. This could be misleading as certain physical phenomena would be ignored. For instance, a significant reduction in molecular weight ($\sim 70\%$ total molecular weight reduction) takes place in this initial short-time regime. Using the approach outlined here, the data can be rationalized as a combination of zeroth- and first-order reactions, where the zeroth-order reaction proceeds initially for time t' , followed by a first-order reaction up to time t . Using eqs 4 and 5, and denoting $M(t) = M$, it follows that

$$\frac{1}{M} - \frac{1}{M_0} = \frac{k}{mN_0}t' \quad (6)$$

and

$$\frac{1}{M(t)} - \frac{1}{M} = \frac{k_1}{m}(t - t') \quad (7)$$

where k and k_1 are the rate constants for the zeroth- and first-order reactions, respectively, and N_0 is the number of molecules in the system. By using eqs 6 and 7, both data sets in Figure 5 can be modeled as a combination of two reactions. (The two broken segments for each curve indicate the model fits.) The above-

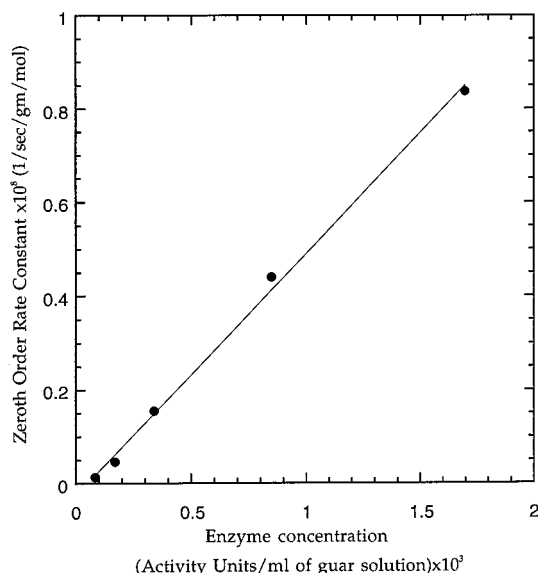


Figure 6. Effect of enzyme concentration on the zero-order rate constant. Degradation was performed on 1% guar samples at 25 °C.

mentioned method can thus be utilized to analyze aspects of the kinetic process previously ignored.

A convenient way to control the kinetics of enzymatic guar hydrolysis is to vary enzyme concentration. Consequently, it is of interest to evaluate the effects of enzyme concentration on the degradation rates and rate constants. Figure 6 reveals that the apparent rate constant increases linearly with initial enzyme concentration ($[E]_0$). Thus, the dependence of molecular weight on enzyme concentration can be accounted for explicitly as

$$\frac{1}{M_t} = \frac{1}{M_0} + \frac{k_0[E]_0}{mN_0}t \quad (8)$$

The functional dependence of molecular weight on enzyme concentration proves to be very useful in deriving scaling relationships for viscosity (as shown later). Since only the initial enzyme concentration appears in the expression for molecular weight reduction, it can also be inferred that the enzyme concentration remains constant throughout the course of degradation. This is consistent with the catalytic nature of enzymatic action and an encouraging corroboration of the data and analyses. It also indicates that the enzyme is not deactivated even after a large number of scission events and corresponding molecular weight reduction. The constant, k_0 , is the number of guar linkages broken per enzyme molecule per unit time and is, thus, a measure of catalytic efficiency. The commercial system contains other proteins in addition to the catalytic protein (enzyme), and the concentration of the enzyme (in mol/L) cannot be determined exactly. As a result, a precise number cannot be ascribed to k_0 , but it was estimated to be of the order of 10.

Reduction of Guar Solution Viscosity upon Enzymatic Degradation. Figure 7 shows a typical viscosity versus shear stress plot of guar solutions tested after different time intervals of degradation by the *Aspergillus* enzyme. The viscosity is significantly reduced as a result of enzymatic hydrolysis, with a 3 order of magnitude decrease after 5 h. For all cases, Newtonian behavior is observed, with viscosity independent of shear stress at low shear stresses (~ 1 dyn/cm²). At higher stresses, guar solutions display shear thinning; i.e., the viscosity decreases with increasing shear stress. The viscosity in the Newtonian region (also termed as zero-shear viscosity) is used to compare samples degraded to different extents.

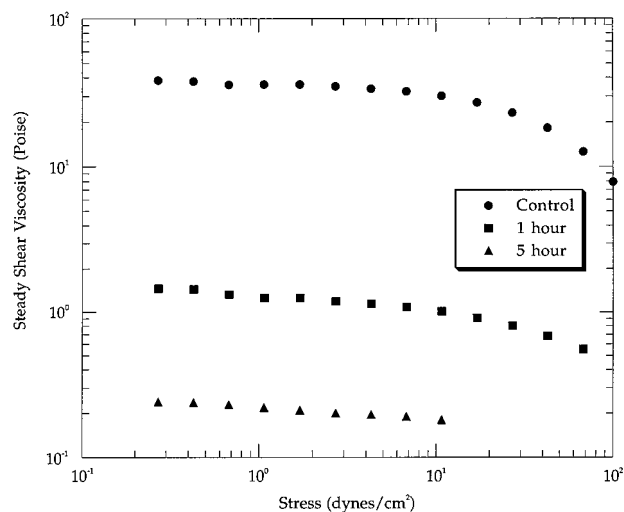


Figure 7. Typical plot of steady shear viscosity as a function of shear stress for guar solutions degraded to different extents. Data shown for 0.7% guar solutions degraded by 2×10^{-4} U of enzyme/mL of guar solution.

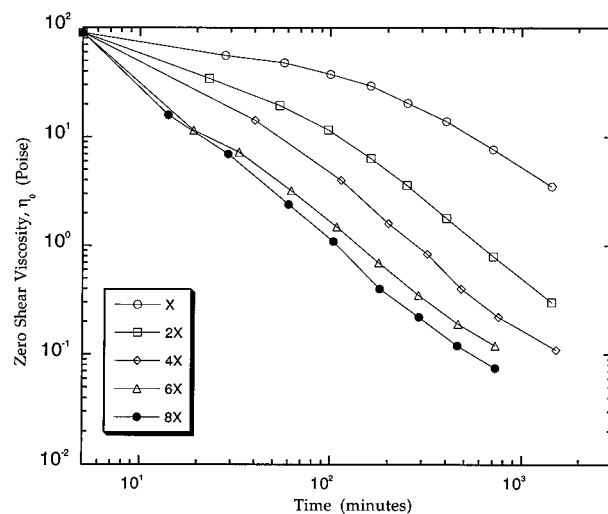


Figure 8. Effect of enzyme concentration on kinetics of reduction in zero shear viscosity for enzymatically degraded guar solutions. Enzyme concentrations ranged from 1.4×10^{-4} (x) to 1.12×10^{-3} (8x) U of enzyme/mL of guar solution. See Appendix for enzyme activity measurements.

nian behavior is observed, with viscosity independent of shear stress at low shear stresses (~ 1 dyn/cm²). At higher stresses, guar solutions display shear thinning; i.e., the viscosity decreases with increasing shear stress. The viscosity in the Newtonian region (also termed as zero-shear viscosity) is used to compare samples degraded to different extents.

Figure 8 shows zero-shear viscosity of enzymatically degraded 1.0% guar solutions, as a function of degradation time for different enzyme concentrations. At all concentrations, a significant reduction is observed. Additionally, the rate of viscosity reduction increases with increasing enzyme concentration. Since the shapes of the viscosity profiles are similar at different enzyme concentrations, the individual profiles could be superimposed by shifting these along the time axis. The results are shown in Figure 9 which plots zero shear viscosity as a function of a reduced time variable $t_r = a_t t$, where a_t is the shift factor required for superposition of the curves. The viscosity profile at an enzyme concentration of x has been chosen as the reference curve;

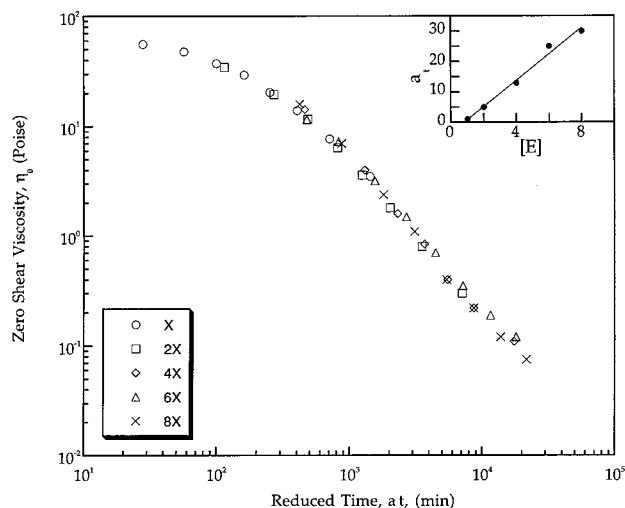


Figure 9. Master curve for the viscosity versus time profiles shown in Figure 8. Inset shows the shift factor required for "best fit" superposition.

hence $a_t = 1$ for $[E] = 1.4 \times 10^{-3}$ U/mL of guar solution. The resultant fit is remarkably good over the entire range of solution viscosity and enzyme concentrations. It is of interest to note that the shift factor a_t varies linearly with enzyme concentration, as shown in the inset of Figure 9.

The successful scaling of the zero-shear viscosity at a given temperature for a specific polymer/enzyme combination during enzymatic hydrolysis can be understood by combining the molecular information obtained from GPC with viscosity results. The molecular weight data from GPC (Figure 3) during enzymatic hydrolysis, expressed mathematically in eq 8, indicates that

$$M = f(Et) \quad (9)$$

i.e., the molecular weight (M) is a function of the product of enzyme concentration $[E]$ and degradation time $[t]$. However, since zero shear viscosity η_0 can be expected to relate uniquely with average molecular weight, we thus anticipate

$$\eta_0 = f(Et) \quad (10)$$

i.e., viscosity is a function of a single variable. Consequently, the viscosity of degraded guar should be superposable by plotting η_0 versus $a_t t$, where a_t accounts for enzyme concentration. Experimentally, we find the shift factor $a_t \sim E$ (see Figure 9), consistent with the first-order dependence of viscosity on enzyme concentration. The scaling is a significant result because it yields a priori prediction of guar solution viscosity for any given enzyme concentration and degradation time.

The results of this initial study provide explicit information on the kinetics of enzymatic degradation, reveal how molecular weight information on polymer degradation studies can be misinterpreted, and unveil a temporal scaling relationship of viscosity. However, there are several critical issues that remain unresolved. Of particular interest are effects of the state of the polymer (solution versus gel) on kinetics and the mechanism of enzymatic degradation. For instance, pathways for enzymatic degradation have been divided into two main groups, single and multiple scission attack.³⁰ In the single scission mode, each encounter between enzyme and substrate results in scission of only one bond.

Table 1

n rxn order	DP ($=M/m$)	% error
0	100	0
	1000	0
2	100	10^{-2}
	1000	10^{-4}
3	100	3×10^{-2}
	1000	3×10^{-4}
5	100	0.1
	1000	0.01

On the other hand, for the multiple attack mode, the enzyme stays attached to one fragment from the initial scission and cleaves additional bonds before dissociating from the substrate molecule. Further work is underway to elucidate these and other issues.

Conclusions

The enzymatic degradation of guar galactomannan was used to demonstrate an important feature in the kinetic analysis of polymer degradation reactions. The inverse relation between molecular weight and time, traditionally considered as evidence for first-order kinetics, was shown to hold regardless of the reaction order. Instead, the dependence of the rate of molecular weight reduction on initial polymer concentration was found to determine the order of the polymer degradation reaction. In particular, for enzymatic hydrolysis of guar, the degradation reaction was found to follow zeroth-order kinetics with respect to guar concentration.

The rheological properties of guar were sensitive to enzymatic hydrolysis, with the zero-shear viscosity exhibiting several orders of magnitude decrease during the course of polymer chain scission. More importantly, the viscosity–time profiles for different enzyme concentrations were collapsed on to a single curve by shifts along the time axis. By doing so, an a priori prediction of guar solution viscosity as a function of degradation time and enzyme concentration could be made. The superposition of the data was possible due to the existence of a unique correlation between degradation time, molecular weight, and viscosity.

Acknowledgment. The authors gratefully acknowledge the U.S. Department of Agriculture and National Science Foundation for financial support of this work. Thanks are also due to Prof. David Ollis for his comments and suggestions during the preparation of this manuscript.

Appendix

For an n th-order reaction ($n \neq 1$), the general relation between molecular weight and time is

$$\left[\left(1 - \frac{m}{M(t)} \right)^{1-n} - \left(1 - \frac{m}{M(0)} \right)^{1-n} \right] = \frac{k(n-1)}{N_0^{1-n}} t$$

The terms on the left-hand side can be expanded as Maclaurin series:

$$\left(1 - \frac{m}{M} \right)^{1-n} = 1 + (n-1) \left(\frac{m}{M} \right) + \text{higher-order terms}$$

By neglecting the higher-order terms, a linear relation between reciprocal of M and time is obtained. Table 1 shows the error by neglecting the higher-order terms.

References and Notes

- (1) Painter, T. J.; Gonzalez, J. J.; Hemmer, P. C. Distribution of D-galactosyl groups in guaran and locust bean gum. *Carbohydr. Res.* **1979**, *69*, 217.
- (2) McCleary, B.; Clark, A.; Dea, I.; Rees, D. The fine structure of carob and guar galactomannans. *Carbohydr. Res.* **1985**, *139*, 237.
- (3) Brant, D. A., Ed. *Solution Properties of Polysaccharides*; ACS Symposium Series No. 150; American Chemical Society: Washington, DC, 1981.
- (4) Shay, G. D. In *Polymers in Aqueous Media: Performance through association*; ACS Symposium Series 223; Glass, J. E., Ed.; American Chemical Society: Washington, DC, 1989; Chapter 25, p 457.
- (5) Bulpin, P. V.; Gidley, M. J.; Jeffcoat, R.; Underwood, D. R. Development of a biotechnological process for the modification of galactomannan polymers with plant α -galactosidase. *Carbohydr. Polym.* **1990**, *12*, 155.
- (6) Prud'homme, R. K.; Constien, V.; Knoll, S. Polymers in aqueous media: Performance through association. Glass, J. E., Ed.; *Adv. Chem. Ser.* **1989**, *223*, 89.
- (7) Kesavan, S.; Prud'homme, R. K. Rheology of guar and HPG crosslinked by borate. *Macromolecules* **1992**, *25*, 2026.
- (8) Pezron, E.; Leibler, L.; Richard, A.; Audebert, R. Reversible gel formation induced by ion complexation. 1. Borax-galactomannan interactions. *Macromolecules* **1988**, *21*, 1121.
- (9) Pezron, E.; Leibler, L.; Richard, A.; Audebert, R. Reversible gel formation induced by ion complexation. 2. Phase diagrams. *Macromolecules* **1988**, *21*, 1128.
- (10) Robinson, G.; Ross-Murphy, S. B.; Morris, E. R. Viscosity-molecular weight relationships, intrinsic chain flexibility, and dynamic solution properties of guar galactomannan. *Carbohydr. Res.* **1982**, *107*, 17.
- (11) Tayal, A.; Kelly, R. M.; Khan, S. A. Viscosity reduction of hydraulic fracturing fluids through enzymatic hydrolysis. *SPE J.* **1997**, *2* (2), 204.
- (12) Whitcomb, P. J.; Gutowski, J.; Howland, W. W. Rheology of guar solutions. *J. Appl. Polym. Sci.* **1980**, *25*, 2815.
- (13) McCleary B. V.; α -D-Galactosidase from lucerne and guar seed. In *Methods in Enzymology*; Willis, W. A., Kellog, S. T., Eds.; Academic Press: San Diego, CA, 1988; Vol. 160, p 627.
- (14) Tayal, A.; Pai, V. B.; Kelly, R. M.; Khan, S. A. Enzymatic Modification of Guar Solutions: Viscosity-Molecular Weight Relationships. In *Water Soluble Polymers: Solution Properties and Applications*; Amjad, Z., Ed.; Plenum Press: New York, 1998.
- (15) Nagy, D. J. Universal calibration in aqueous size exclusion chromatography with on-line differential viscometry using commercial TSK-PW columns. *J. Liq. Chromatogr.* **1990**, *13* (4), 677.
- (16) Kato, T.; Okamoto, T.; Tokuy, T.; Takahashi, A. Solution properties and chain flexibility of pullulan in aqueous solution. *Biopolymers* **1982**, *21*, 1623.
- (17) Ekenstam, A. af, über das verhalten der cellulose in mineral-säure-lösungen, I. Mitteil.: Die bestimmung des molekular-gewichts in phosphorsäure-lösung. *Ber. Dtsch. Chem. Ges.* **1936** (69), 553.
- (18) Simha, R. Kinetics of degradation and size distribution of long chain polymers. *J. Appl. Phys.* **1941**, *12*, 569.
- (19) Davis, A.; Golden, J. H. Degradation of polycarbonates III. Viscometric study of thermally induced chain scission. *Die Makromol. Chem.* **1964** (78), 16.
- (20) Singh, S. K.; Jacobsson, S. P. Kinetics of acid hydrolysis of κ -carrageenan as determined by molecular weight (SEC-MALLS-RI), gel breaking strength, and viscosity measurements. *Carbohydr. Polym.* **1994**, *23*, 89.
- (21) McBurney, L. F. Degradation of Cellulose. In *Cellulose and Cellulose Derivatives*, 2nd ed.; Ott, E., Spurlin, H., Graffin, M., Eds.; Interscience Publishers: New York, 1954; Vol. 99.
- (22) Ravens, D. A. S.; Sisley, E. J. Cleavage Reactions. In *Chemical Reactions of Polymers*; Fettes, E. M., Ed.; Interscience Publishers: New York, 1964; Vol. 551.
- (23) Figini, M. M. The acid-catalyzed degradation of cellulose linters in distinct ranges of degree of polymerization. *J. Appl. Polym. Sci.* **1987**, *33*, 2097.
- (24) Masson, C. R. The degradation of Carrageenan I. Kinetics in aqueous solution at pH 7. *Can. J. Chem.* **1955**, *33*, 597.
- (25) Masson, C. R.; Santry, D.; Caines, G. W. The degradation of Carrageenan II. Influence of further variables. *Can. J. Chem.* **1955**, *33*, 1088.
- (26) Graessley, W. W. Viscoelasticity and flow in polymer melts and concentrated solutions. In *Physical Properties of Polymers*; Mark, J. E., Ed.; 2nd ed.; American Chemical Society: Washington, DC, 1993.
- (27) Basedow, A. M.; Ebert, K. H.; Ederer, H. J. Kinetic studies on the acid hydrolysis of dextran. *Macromolecules* **1978**, *11*, 774.
- (28) Eriksson, K. E.; Winell, M. Purification and characterization of a fungal β -mannanase. *Acta Chem. Scand.* **1968**, *22*, 1924.
- (29) McCleary, B. V.; Matheson, N. M. Action patterns and substrate-binding requirements of β -D-mannanase with mannosaccharides and mannan type polysaccharides. *Carbohydr. Res.* **1983**, *119*, 191.
- (30) Azhari, R.; Lotan, N. Enzymic depolymerization processes: reaction pathways as a basis for a new classification and nomenclature. *J. Mater. Sci. Lett.* **1991**, *10*, 243.

MA980773W